Hindawi
Advances in Civil Engineering
Volume 2019, Article ID 9747896, 8 pages
https://doi.org/10.1155/2019/9747896

Research Article

The Effect of Concrete Footing Shape in Differential Settlement: A Seismic Design

Abdoullah Namdar, Yun Dong, and Yin Deyu

Faculty of Architecture and Civil Engineering, Huaiyin Institute of Technology, Huai'an, China

Correspondence should be addressed to Yun Dong; hadyun@163.com

Received 30 December 2018; Accepted 21 February 2019; Published 10 April 2019

Guest Editor: Edén Bojórquez

This paper presents the numerical results of concrete footing-soil foundation seismic interaction mechanism. The concrete footing has been made with two different shapes, but with the equal volume of concrete material. The concrete footing-soil foundation has been analyzed using nonlinear finite elements, with the fixed-base state. The simulated near-fault ground motions have been applied to the concrete footing-soil foundation. The problem has been formulated based on the settlement controlled analysis. The local geotechnical conditions of all configurations have been analyzed. The numerical analysis results indicate that the shape of a concrete footing alters seismic response, revises inertial interaction, enhances damping ratio, improves load carry capacity, modifies cyclic differential settlement, revises failure patterns, minimizes nonlinear deformation, and changes cyclic strain energy dissipation. The novelty of this research work is the strain energy has more been dissipated with artistic concrete footing design.

1. Introduction

A number of the buildings have been collapsed due to improper soil-footing interaction; it has occurred when dynamic or seismic forces have been applied to them. The improvement of soil-footing seismic interaction mechanism is an art in geotechnical earthquake engineering design and needs to select appropriate footing shape to enhance the safety of the structure.

There are many experimental, numerical, and theoretical research studies which mainly focus on differential settlement and bearing capacity of the soil when the soil has been subjected to simulated seismic loading, liquefaction, and landslide. The outcome of these research studies has been realizing failure mitigation of soil foundation and introducing different methods for improving soil foundation stability [1–12]. Using research idea from different branches of science and applying them in geotechnical earthquake engineering is an acceptable research methodology. In this regard, there is an investigation on quantitative shape evaluation of graphite particles in ductile iron [13]; with attention to this research work, the effect of concrete footing shape in minimizing differential settlement of soil foundation needs to be investigated. However, the geotechnical earthquake engineering is a young field, and the concept of the seismic stress response of concrete footing-soil foundation model is a complicated mechanism and needs more investigation. In the present study, the seismic design of concrete footing with considering the configuration of concrete footing to minimize differential settlement at the base of concrete footing has been investigated. Earthquake includes differential settlement, but the shape of concrete footing in producing differential settlement has not been studied with considering seismic response at the base of a concrete footing, energy dissipation, hysteretic soil damping, strain travel paths, inertial interaction, nonlinear deformation patterns, and footing-soil seismic interaction mechanism. We hope all we have done could support the seismic design of concrete footing in considering the safety of concrete footing and soil foundation to support solving geotechnical earthquake engineering problems.

2. Problem Definition

In the previous studies, many investigations have been made in understanding the differential settlement of soil, when the

soil has been subjected to dynamic loading [2, 3, 6, 12]. The present investigations analyzed the soil foundation-concrete footing seismic interaction mechanism and stability, with considering concrete shape. There is no investigation on the effect of concrete footing geometry to soil foundation-concrete footing seismic interaction present in the literature, and the associated simulation indirectly even cannot be found in the literature. The idea to do this research work is to understand the effect of concrete footing shape on (i) soil foundation-concrete footing seismic interaction mechanism, (ii) the differential settlement, (iii) the nonlinear deformation, (iv) the strain paths, and (v) the failure patterns. Two types of concrete foundations have been considered and have been analyzed numerically. The concrete footing and soil foundation, simultaneously, have been subjected to seismic loading. In all configurations, single concrete footing has been analyzed. In the present study, the specific geometry of concrete footing may increase or reduce soil-footing interaction. From the theoretical concept point of view, to provide an appropriate solution for this problem, and for solving and demonstrating this elasticity problem, the ABAQUS software has been employed. The ABAQUS has been employed to solve and explain many engineering problems in the various fields through numerical simulation [12, 14–18]. The ABAQUS has the ability to solve nonlinear problems in high quality. To design the concrete footing with maximum safety and minimum cost, two different configurations of concrete footing have numerically been investigated. In both configurations, the same volume and grade of concrete have been used. The method of embedded concrete footing in the soil foundation is adopted, and also the interaction method for soil foundation with concrete footing in ABAQUS environment has been adopted. The footing and soil have been loaded. The problem has been formulated based on the settlement controlled analysis. The seismic response of concrete footing and soil foundation in all models has been compared.

3. Domain Theoretical Concept for Present Analysis

The nonlinear deformation develops due to six components of stresses applied to a body element; the six components of stresses are $\sigma_x, \sigma_y, \sigma_z, \tau_{xy}, \tau_{xz}$, and τ_{yz}.

Two types of distortions arise: (i) direct strain $\varepsilon_x, \varepsilon_y$, and ε_{yz} from σ_x, σ_y, and σ_z and (ii) angular distortions e_{xy}, e_{xz}, and e_{yz} from τ_{xy}, τ_{xz}, and τ_{yz}. The strains and rotation components for each tensor may be expressed in terms of their respective displacements gradients:

$$e_{ij} = \begin{bmatrix} \dfrac{\partial u}{\partial x} & \dfrac{\partial u}{\partial y} & \dfrac{\partial u}{\partial z} \\ \dfrac{\partial v}{\partial x} & \dfrac{\partial v}{\partial y} & \dfrac{\partial v}{\partial z} \\ \dfrac{\partial w}{\partial x} & \dfrac{\partial w}{\partial y} & \dfrac{\partial w}{\partial z} \end{bmatrix}. \quad (1)$$

The strain matrix is

$$\varepsilon_{ij} = \begin{bmatrix} \dfrac{\partial u}{\partial x} & \dfrac{1}{2}\left(\dfrac{\partial u}{\partial y} + \dfrac{\partial v}{\partial x}\right) & \dfrac{1}{2}\left(\dfrac{\partial u}{\partial z} + \dfrac{\partial w}{\partial x}\right) \\ \dfrac{1}{2}\left(\dfrac{\partial u}{\partial y} + \dfrac{\partial v}{\partial x}\right) & \dfrac{\partial v}{\partial y} & \dfrac{1}{2}\left(\dfrac{\partial v}{\partial z} + \dfrac{\partial w}{\partial y}\right) \\ \dfrac{1}{2}\left(\dfrac{\partial u}{\partial z} + \dfrac{\partial w}{\partial x}\right) & \dfrac{1}{2}\left(\dfrac{\partial v}{\partial z} + \dfrac{\partial w}{\partial y}\right) & \dfrac{\partial w}{\partial z} \end{bmatrix}. \quad (2)$$

The rotation matrix is

$$\omega_{ij} = \begin{bmatrix} 0 & \dfrac{1}{2}\left(\dfrac{\partial u}{\partial y} - \dfrac{\partial v}{\partial x}\right) & \dfrac{1}{2}\left(\dfrac{\partial u}{\partial z} - \dfrac{\partial w}{\partial x}\right) \\ -\dfrac{1}{2}\left(\dfrac{\partial u}{\partial y} - \dfrac{\partial v}{\partial x}\right) & 0 & \dfrac{1}{2}\left(\dfrac{\partial v}{\partial z} - \dfrac{\partial w}{\partial y}\right) \\ -\dfrac{1}{2}\left(\dfrac{\partial u}{\partial z} - \dfrac{\partial w}{\partial x}\right) & -\dfrac{1}{2}\left(\dfrac{\partial v}{\partial z} - \dfrac{\partial w}{\partial y}\right) & 0 \end{bmatrix},$$

$$\begin{bmatrix} e_x & e_{xy} & e_{xz} \\ e_{yx} & e_y & e_{yz} \\ e_{zx} & e_{zy} & e_z \end{bmatrix} = \begin{bmatrix} \varepsilon_x & \varepsilon_{xy} & \varepsilon_{xz} \\ \varepsilon_{yx} & \varepsilon_y & \varepsilon_{yz} \\ \varepsilon_{zx} & \varepsilon_{zy} & \varepsilon_z \end{bmatrix} + \begin{bmatrix} \omega_x & \omega_{xy} & \omega_{xz} \\ \omega_{yx} & \omega_y & \omega_{yz} \\ \omega_{zx} & \omega_{zy} & \omega_z \end{bmatrix}. \quad (3)$$

Consequently, the complete distortion of a volume element may be expressed as the sum of corresponding strains and rotations in the matrix form [19]. In this study, the nonlinear finite element analysis has been applied to analyze seismic behavior of concrete footing-soil foundation interaction. Accordingly, the soil foundation and concrete footing have numerically been investigated. The six strain components will not act independently; they have a direct relationship with the displacements. Under earthquake function, due to loading, unloading, and reloading process, an element can translate, rotate, compress, or elongate.

4. Materials and Modeling

The concrete footing-soil foundation has been modeled using nonlinear finite elements, with the fixed-base state. The soil foundation is $1.8 * 1.8 * 0.9$ (m). The concrete footing for configuration-1 and configuration-2 are $0.6 * 0.6 * 0.4$ (m) and $0.4 * 0.9 * 0.4$ (m), respectively. For both models, the concrete foundation of $0.2 * 0.2 * 0.2$ (m) is installed on center of concrete footing. The soil foundation-concrete footing seismic interaction has been evaluated. The concrete footing configuration is with two different shapes and equal volume. In the numerical analysis, the typical mesh has been used. The concrete footing is placed on a horizontal surface of the soil foundation; it is shown in Figures 1 and 2. The simulated near-fault ground motions, with equal magnitude, have numerically been applied to concrete footing and soil foundation. The acceleration history of the earthquake occurred in Norcia, Italy, has been used in numerical analysis and is shown in Figures 3 and 4. From 22 to 28 seconds of the earthquake, the main seismic excitation has been observed. In comparing E, N, and Z comps, the E comp has maximum acceleration history and

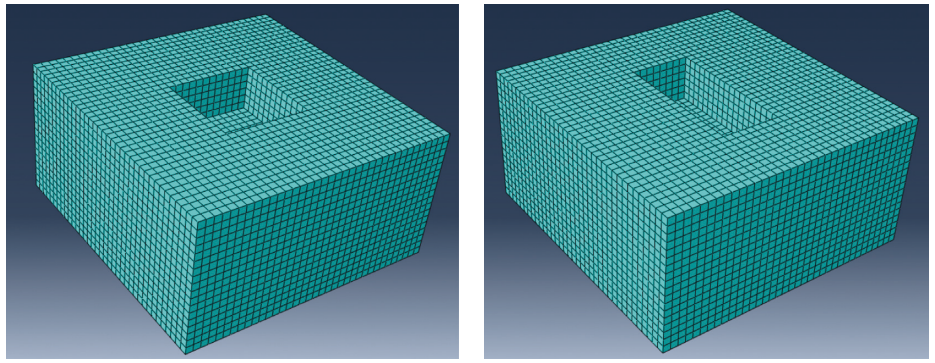

(a) (b)

Figure 1: Soil models. (a) Configuration-1. (b) Configuration-2.

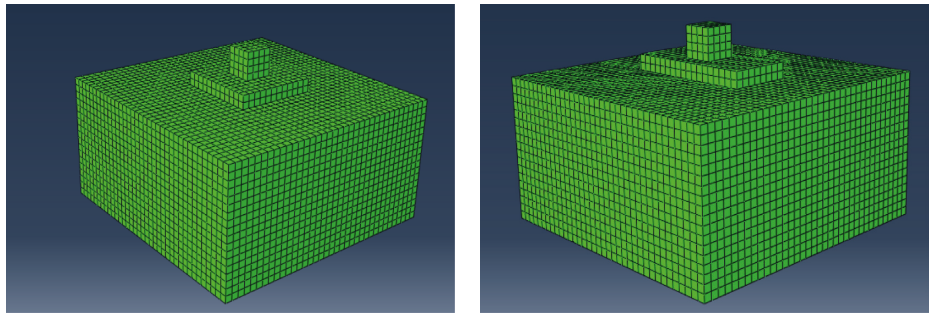

(a) (b)

Figure 2: Concrete footing-soil configurations. (a) Configuration-1. (b) Configuration-2.

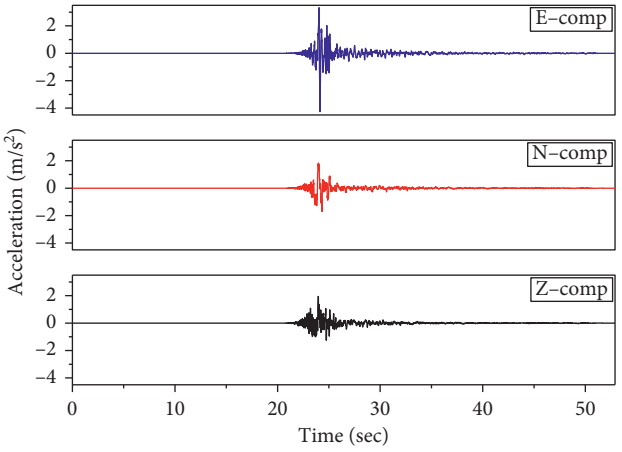

Figure 3: Acceleration history of Norcia Earthquake [20].

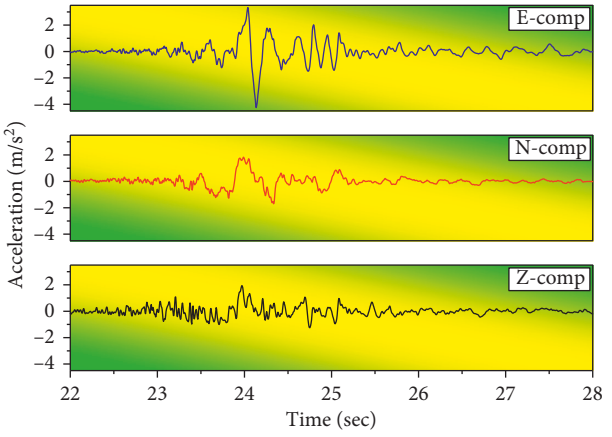

Figure 4: Acceleration history of Norcia Earthquake [20].

nonlinearity tolerance in Norcia Earthquake. However, due to these reasons, the E comp has been selected for numerical analysis. The mechanical properties of materials have been used in this analysis, extracted from those reported in the literature, and are shown in Table 1. The soil is often discretized with solid finite elements. Nonlinear numerical analysis has been performed based on realistic seismic data. The earthquake data have been used in numerical analysis and are reported by AMATRICE station, with 8.9 (km) distance from the epicenter of the earthquake. The Norcia Earthquake occurred with 6.2 magnitude, at the location of 42.71 N 13.17 E, and depth of 10.0 km, on 1 : 36 : 33 UTC, 24 August 2016.

5. Numerical Analysis, Discussion, and Verification of the Result

Enhancement geometry of a concrete footing considerably changes soil-footing seismic interaction mechanism, and this process leads to develop a new concept for the satisfactory seismic design of a concrete footing. The morphology

Table 1: Mechanical properties of materials [21, 22].

Materials	Modulus elasticity, E (MPa)	Poisson's ratio, (ν)	Friction angle, ϕ (degree)	Dilatancy angle, ψ (degree)	Cohesion, c (kPa)	Unit weight, γ (kN/m^3)	Ref
Soil	120	0.35	53	21	0.01	22.68	[21]
Concrete	49195	0.24	—	—	—	24.405	[22]

of concrete footing influences on the shear strain travel paths and seismic energy distribution. The meaningful relationships have been observed between simulated near-fault ground-shaking and energy dissipation mechanism at each configuration. The characteristics of seismic waves are altered as it is facing different simulated geomorphological conditions. The seismic wave dispersion modifies damping ratio and governs nonlinear deformation patterns of soil foundation and footing-soil seismic interaction mechanism. However, the morphology of concrete footing significantly affects the amplitude of earthquake ground motions; it may be known as "geomorphological conditions effect" in concrete footing-soil foundation seismic design. The numerical analysis results have confirmed that the geomorphological condition influence to strain energy dissipation, and this process leads to developing nonlinear deformation patterns and differential settlement with the specific shape at each configuration, and subsequently, it is understood that the geomorphological conditions are important in the distribution of earthquake damage. The flexible soil foundation area-to-ridge concrete footing area interaction is responsible for the failure mechanism of soil foundation at each configuration. However, the design of concrete footing shape at each configuration is important in the stability of concrete footing and soil foundation as well. The modified shape of concrete footing leads to change in the concrete footing center of gravity and shape of cyclic load distribution; this phenomenon results in the modification of concrete footing-soil foundation seismic interaction mechanism and seismic load response. And on the other hand, the geomorphological conditions and morphology of concrete footing are responsible for developing characteristics of strain paths, and the strain path is a factor in developing a differential settlement, failure mechanism, deformation, and bearing capacity. The seismic site response is highly variable with respect to concrete footing morphology, while the volume of used concrete is equal in both configurations, and cost effectiveness of the project is considered with seismic design of concrete footing. The geotechnical condition is another factor in ground motion behavior prediction. The geomorphological condition affects the seismic response of an infrastructure. It can suggest beyond the theoretical seismic design; it requires to numerically simulate the influence of geomorphological conditions to predict seismic stability of the infrastructure. The near-fault ground motions change strain energy dissipation via travel path of seismic wave propagation. The hysteretic behavior of soil significantly affects the concrete footing seismic response. This process affects concrete footing and soil foundation inertial interaction and leads to stress response of the soil foundation. Cyclic seismic load response has been developed due to concrete footing morphology, and it is shown in Figures 5 and 6. The seismic loading and concrete footing

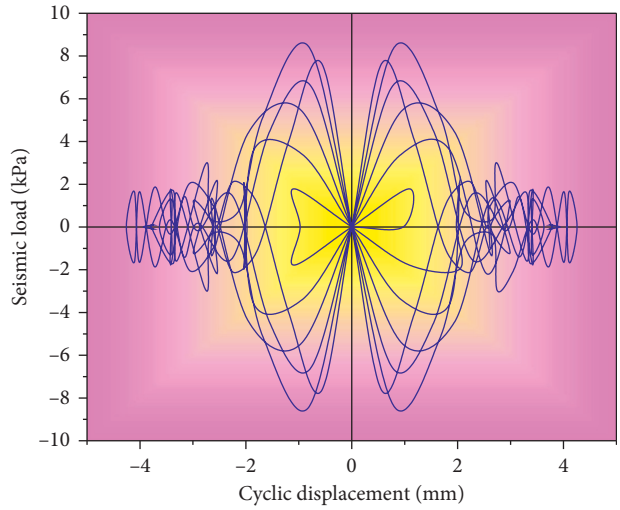

Figure 5: Seismic load (kPa) vs cyclic displacement (mm) at the base of a concrete footing, configuration-1.

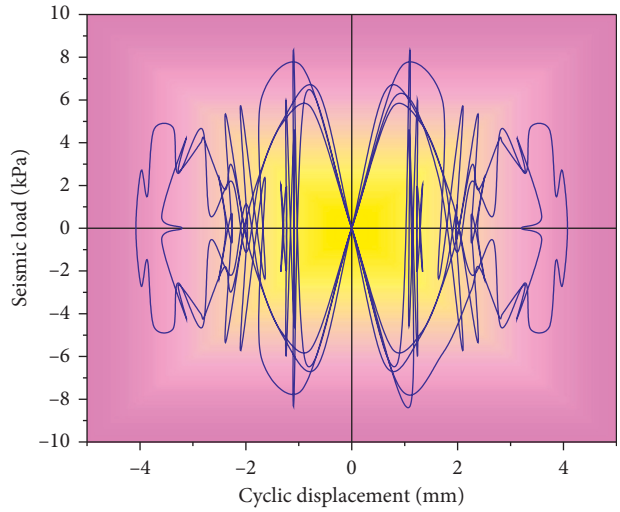

Figure 6: Seismic load (kPa) vs cyclic displacement (mm) at the base of a concrete footing, configuration-2.

morphology are responsible for soil compaction, modify soil foundation shear strength, and alter concrete footing-soil foundation seismic interaction mechanism. The geomorphological conditions affect wave motion behavior, and it causes differential ground deformation and differential rotations of concrete footing along its base to interact with soil foundation. The wave energy propagates in different directions and results in forming cyclic volumetric strain and produces nonlinear deformation for each configuration; it is shown in Figures 7 and 8. In configurations 1 and 2, the different ground motions response has been observed; it

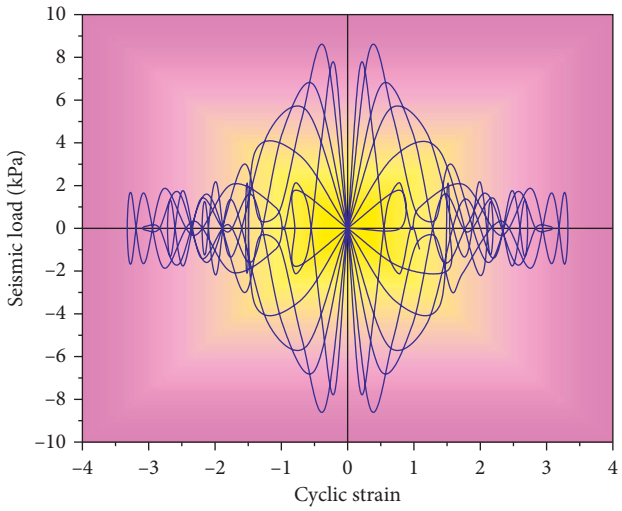

Figure 7: Seismic load (kPa) vs cyclic strain at the base of a concrete footing, configuration-1.

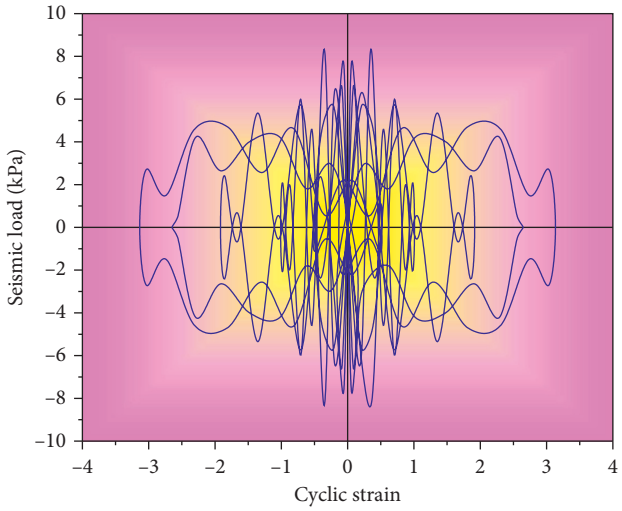

Figure 8: Seismic load (kPa) vs cyclic strain at the base of a concrete footing, configuration-2.

developed with respect to concrete footing shape, and this phenomenon supports in earthquake damage estimation, when the movement of seismic wave radiates along the base and sides of the concrete footing. The seismic wave radiate dislocates the concrete footing at any possible directions, and this phenomenon results in accelerating model and releasing cyclic strain energy. The hysteretic energy dissipation is scattered in all configurations, with the critical mechanism in respect to the flexible the soil foundation area-to-the ridge concrete footing area interaction; this mechanism is responsible for failure mechanism of soil foundation at each configuration. Inertia has been developed due to near-fault ground motions applied to each configuration; it has appeared in the form of base shear, moment, and torsional excitation and causes differential displacements and nonlinear deformation rotation, with a different magnitude in respect to the soil foundation flexibility and concrete footing shape. The damping ratio in configuration-2 is reduced by 15% compared to configuration-1. The shape of concrete footing governs hysteretic soil damping and inertial interaction; this process occurs based on kinematic interaction of concrete footing-soil foundation characteristics and causes concrete foundation motions in soil foundation. The nonlinear deformation significantly influences the overall concrete footing seismic behavior, especially with respect to damping and seismic degrees of damage.

The stress third invariant behavior is depicted in Figures 9–12. A comparative numerical analysis of the seismic response between two differently shaped and equal volume of concrete footing under significantly invariant stresses through establishing nonlinear finite element analysis has been made. The stress third invariant at the base of concrete footing for configuration-1 is formed with higher strain energy and lower energy dissipation magnitude compared to configuration-2. This complex mechanism influences load carry capacity of soil foundation and types of earthquake damage. The evaluated results show that the shearing resistance at configuration-2 is improved due to lower degradation of soil by cyclic loading. The nonlinear seismic load-cyclic strain curve expresses the variation of stiffness and shear strength at the base of the concrete footing. The cyclic strain energy causes increasing nonlinear shear deformation and soil foundation failure if cyclic shear stress increases more than the shear strength of the soil foundation. Figure 9 shows the stress invariant at the base of concrete footing for configurations 1 and 2. As a result, the cyclic strain behavior would be expected to provide a more reliable prediction of differential settlement, in considering concrete footing-soil foundation seismic interaction. The nonlinear seismic load-cyclic strain relationship at both configurations shows the higher strain energy concentration is developed at the base of the configuration-1, with respect to the magnitude and shape of the seismic loading. However, the differential settlement is significantly minimized in configuration-2. The higher cyclic strain energy concentration has a direct relationship with nonlinear shear deformation and nonlinear volume change. The failure patterns are plotted in Figure 9, in such a way that red and blue zone implies a fully plastic state. Due to the nature of cyclic loading, nonplastic deformation occurred in any possible direction. The geometry of the failure patterns shows the plastic slice has been occupied more area in configuration-1. The plastic deformation morphology shows that the differential settlement for both models is not the same, and a higher magnitude of differential settlement occurred in configuration-1.

Figures 10 and 11 show the cyclic stress behavior of the configurations 1 and 2 in respect to the size and shape of the plastic deformation. And it describes increment of cyclic stress invariant. The stronger response of earthquake shaking in the configuration-1 has been observed. However, it is a possibility for permanent deformation in configuration-1. The strong strain in several parts of the configuration-1 results in permanent nonlinear shear deformations and nonlinear volume change. The nonlinear volumetric strain often refers to ground failure. It is the

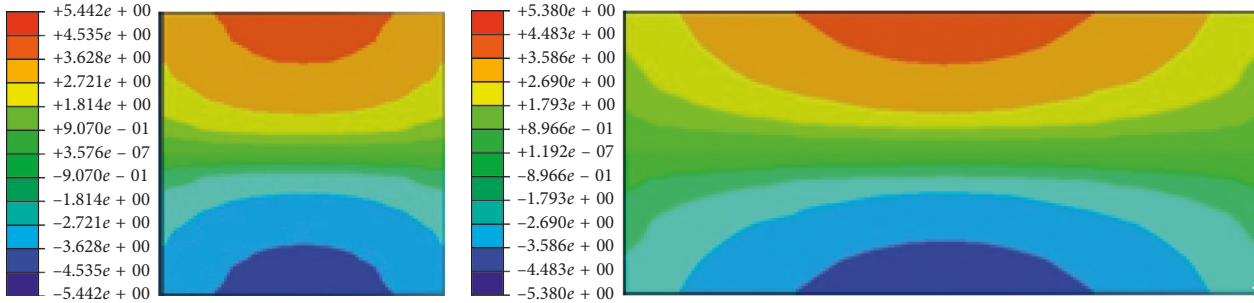

Figure 9: Cyclic stress invariant at the base of the concrete footing. (a) Configuration-1. (b) Configuration-2.

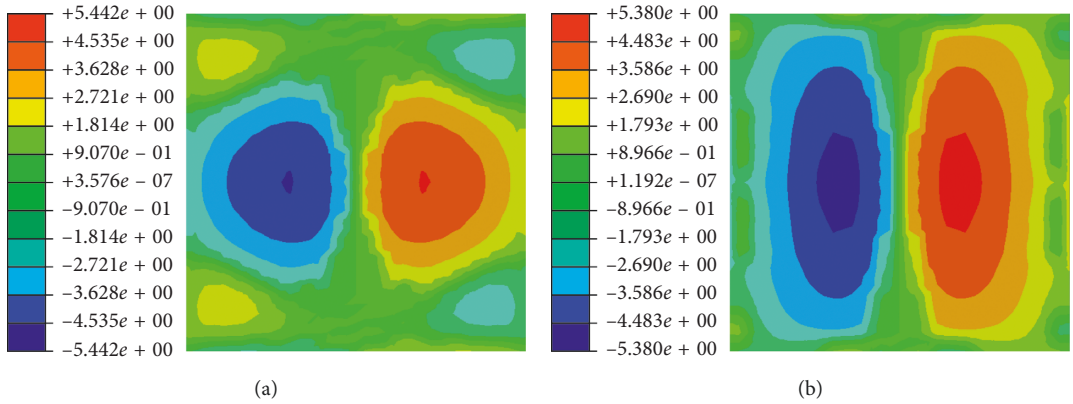

Figure 10: Cyclic stress invariant at the base of the soil foundation. (a) Configuration-1. (b) Configuration-2.

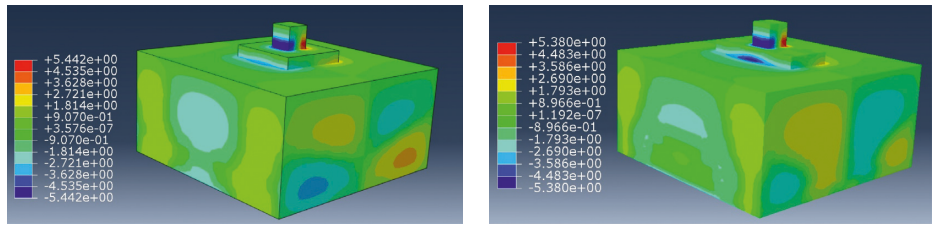

Figure 11: Cyclic stress invariant for configurations 1 and 2. (a) Configuration-1. (b) Configuration-2.

possibility of ground failure in the form of lateral ground displacement, and it can contribute to the failure of the soil foundation.

Color map surface projection techniques are used in matrix analysis to simulate results of ABAQUS software, which is reported in cyclic stress invariant. According to Figure 12, by using the matrix in numerical simulation, the development of cyclic stress invariant due to seismic acceleration load response at the base of the soil foundation is illustrated. Figure 12 shows the seismic load travel paths and seismic load directions. The loading and reloading process has been depicted in different colors. The load distribution among two soil foundations is varied; configuration-2 is subjected to more distributed cyclic load compared to configuration-1; it is a result of increasing stable soil-concrete footing interaction in configuration-2. It can be concluded that the stability of configuration-2 is higher than configuration-1.

The minimum strain energy density allows the influence of the T-stress on the mixed modes I/II fracture strength [23]. And the specimen geometry can strongly influence the mode-I fracture strength [24]. The hysteretic energy dissipation influences the flexible soil foundation area-to-the ridge concrete footing area interaction and governs failure mechanism. The configurations 1 and 2 affect strain energy dissipation, according to their geometry. The results of the numerical analysis show good agreements with those reported in the literature.

The different types of loads can store elastic energy before damage, and this energy storage accelerates and develops damage mechanism [25–33]. In the present numerical analysis, it has been observed that the shape of

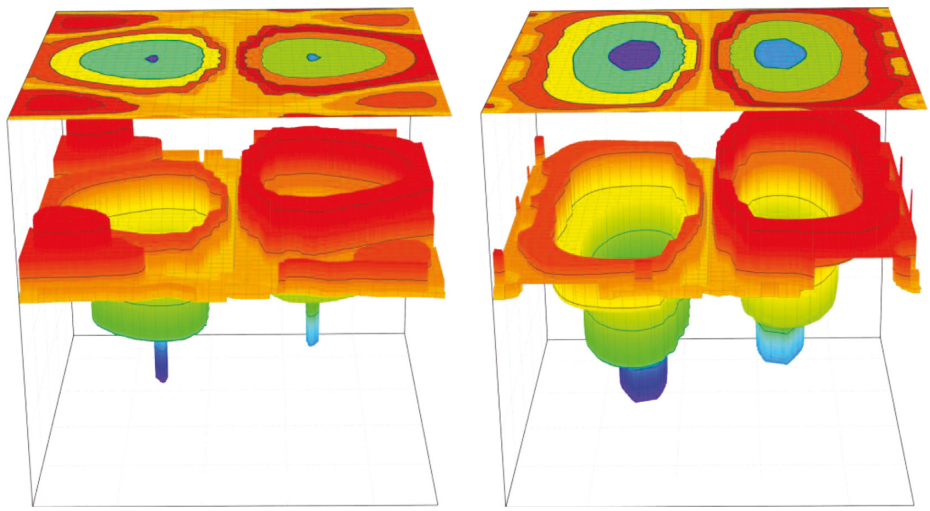

(a) (b)

Figure 12: 3D cyclic stress invariant of soil at the base of soil foundation, using matrix for numerical simulation. (a) Configuration-1. (b) Configuration-2.

concrete footing causes storage strain energy mechanism and strain energy dissipation as well. The cyclic strain energy causes deformation, with respect to the shape of the concrete footing. The soil foundation was subjected to the seismic excitation and deforms. This deformation occurs according to an internal energy mechanism and concrete footing shape. This internal energy is known as strain energy. In the present study, the strain energy has more been dissipated with artistic concrete footing design. The configuration of soil foundation-concrete footing significantly modified strain energy storage and damage patterns. The stress component distribution due to the external forces depends on the strain energy function. However, the shape of concrete footing directly affects seismic acceleration response, damping mechanism, energy dissipation, load carry capacity, differential settlement, nonlinear deformation, strain-stress travel paths, and inertial interaction.

6. Conclusion

The nonlinear finite elements are applied in the analysis of concrete footing-soil seismic interaction mechanism. The concrete footing is built up with two different shapes and equal volume. The simulated near-fault ground motions have been applied to each configuration. In the present study, the following aims have been achieved:

(i) It has been found that the concrete footing-soil interaction and morphology of differential settlement have been changed with respect to the shape of the concrete footing.

(ii) The local geotechnical conditions have been modified ground-shaking characteristics. The anomalous damage distributions may not derive with the select appropriate shape of a concrete footing, considering local site conditions.

(iii) The morphology of concrete footing affects the seismic energy travel paths, and meaningful relationships have been observed between simulated near-fault ground-shaking and energy dissipation mechanism. The strain energy has more been dissipated with artistic concrete footing design.

(iv) The shape of concrete footing governs hysteretic soil damping and inertial interaction; these processes have occurred based on kinematic interaction of concrete footing-soil foundation characteristics.

(v) The higher strain energy concentration has been observed at the base of the configuration-1, with respect to the magnitude and shape of the seismic loading response. The differential settlement is significantly minimized in configuration-2.

(vi) The cyclic strain causes plastic cyclic deformation, with respect to the shape of concrete footing and related to increment of stress. According to the numerical results, this approach supports in forecasting the seismic stability of concrete footing.

Data Availability

No data were used to support this study.

Conflicts of Interest

The authors declare that they have no conflicts of interest.

Acknowledgments

The support by the Major Projects of Natural Science Research in Jiangsu Colleges and Universities (grant no. 17KJA560001), the Science and Technology Planning Project of Jiangsu Province (grant no. BY2016061-29), the Jiangsu Province Six Talent Peak High-Level Talent Project (grant no. JZ-011), and the New Wall Materials and Development of Bulk Cement Projects of Jiangsu Economic and Information Commission (grant no. 2017-21) is greatly acknowledged.

References

[1] A. Namdar and M. K. Pelkoo, "Numerical analysis of soil bearing capacity by changing soil characteristics," *Frattura ed Integrità Strutturale*, vol. 3, no. 10, pp. 38–42, 2009.

[2] A. Namdar, "Liquefaction zone and differential settlement of cohesionless soil subjected to dynamic loading," *EJGE*, vol. 21, no. 2, pp. 593–605, 2016.

[3] A. Namdar and G. S. Gopalakrishna, "Seismic mitigation of embankment by using dense zone in subsoil," *Emirates Journal for Engineering Research*, vol. 13, no. 3, pp. 55–61, 2008.

[4] O. F. Drbe and M. H. El Naggar, "Axial monotonic and cyclic compression behaviour of hollow-bar micropiles," *Canadian Geotechnical Journal*, vol. 52, no. 4, pp. 426–441, 2014.

[5] A. V. Rose, R. N. Taylor, and M. H. El Naggar, "Numerical modelling of perimeter pile groups in clay," *Canadian Geotechnical Journal*, vol. 50, no. 3, pp. 250–258, 2013.

[6] A. Namdar, "Tsunami and liquefaction resistance of subsoil," *Electronic Journal of Geotechnical Engineering*, vol. 18, pp. 5907–5919, 2013.

[7] H. Toyota and S. Takada, "Geotechnical distinction of landslides induced by near-field earthquakes in niigata, Japan," *Geography Journal*, vol. 2015, Article ID 359047, 11 pages, 2015.

[8] A. Y. Abd Elaziz and M. H. El Naggar, "Geotechnical capacity of hollow-bar micropiles in cohesive soils," *Canadian Geotechnical Journal*, vol. 51, no. 10, pp. 1123–1138, 2014.

[9] A. M. Alnuaim, M. H. El Naggar, and H. El Naggar, "Numerical investigation of the performance of micropiled rafts in sand," *Computers and Geotechnics*, vol. 77, pp. 91–105, 2016.

[10] J. Kumar and V. B. K. Mohan Rao, "Seismic bearing capacity factors for spread foundations," *Géotechnique*, vol. 52, no. 2, pp. 79–88, 2002.

[11] D. Chakraborty and J. Kumar, "Seismic bearing capacity of shallow embedded foundations on a sloping ground surface," *International Journal of Geomechanics*, vol. 15, no. 1, article 04014035, 2015.

[12] A. Namdar, "A numerical investigation on soil-concrete foundation interaction," *Procedia Structural Integrity*, vol. 2, pp. 2803–2809, 2016.

[13] A. D. Santis, O. D. Bartolomeo, D. Iacoviello, and F. Iacoviello, "Quantitative shape evaluation of graphite particles in ductile iron," *Journal of Materials Processing Technology*, vol. 196, no. 1–3, pp. 292–302, 2008.

[14] A. Namdar, E. Darvishi, X. Feng, and Q. Ge, "Seismic resistance of timber structure—a state of the art design," *Procedia Structural Integrity*, vol. 2, pp. 2750–2756, 2016.

[15] R. Ali, Q. Z. Khan, and A. Ahmad, "Numerical investigation of load-carrying capacity of GFRP-reinforced rectangular concrete members using CDP model in ABAQUS," *Advances in Civil Engineering*, vol. 2019, Article ID 1745341, 21 pages, 2019.

[16] A. Namdar, Y. Dong, and Y. Liu, "The effect of nonlinearly of acceleration histories to timber beam seismic response," *Material Design and Processing Communication*, 2019, In press.

[17] S. Frank, Ó. R. Ramos, J. P. Reyes, and M. J. Pantaleón, "Relative displacement method for track-structure interaction," *The Scientific World Journal*, vol. 2014, Article ID 397515, 7 pages, 2014.

[18] A. S. Genikomsou and M. A. Polak, "Finite element analysis of punching shear of concrete slabs using damaged plasticity model in ABAQUS," *Engineering Structures*, vol. 98, pp. 38–48, 2015.

[19] D. W. A. Rees, *Basic Engineering Plasticity*, Elsevier, Amsterdam, Netherlands, 2006.

[20] https://strongmotioncenter.org/.

[21] Y. Yu, R. J. Bathurst, and T. M. Allen, "Numerical modelling of two full-scale reinforced soil wrapped-face walls," *Geotextiles and Geomembranes*, vol. 45, no. 4, pp. 237–249, 2017.

[22] J. Li, C. Wu, and H. Hao, "An experimental and numerical study of reinforced ultra-high performance concrete slabs under blast loads," *Materials & Design*, vol. 82, pp. 64–76, 2015.

[23] M. R. Ayatollahi, M. Rashidi Moghaddam, and F. Berto, "A generalized strain energy density criterion for mixed mode fracture analysis in brittle and quasi-brittle materials," *Theoretical and Applied Fracture Mechanics*, vol. 79, pp. 70–76, 2015.

[24] M. R. Ayatollahi, M. Rashidi Moghaddam, S. M. J. Razavi, and F. Berto, "Geometry effects on fracture trajectory of PMMA samples under pure mode-I loading," *Engineering Fracture Mechanics*, vol. 163, pp. 449–461, 2016.

[25] S. You, H. Ji, Z. Zhang, and C. Zhang, "Damage evaluation for rock burst proneness of deep hard rock under triaxial cyclic loading," *Advances in Civil Engineering*, vol. 2018, Article ID 8193638, 7 pages, 2018.

[26] L. Chen, L. Qiao, J. Yang, and Q. Li, "Laboratory investigation of energy propagation and scattering characteristics in cylindrical rock specimens," *Advances in Civil Engineering*, vol. 2018, Article ID 2052781, 7 pages, 2018.

[27] Z. Wang, J. Yao, N. Tian, J. Zheng, and P. Gao, "Mechanical behavior and damage evolution for granite subjected to cyclic loading," *Advances in Materials Science and Engineering*, vol. 2018, Article ID 4312494, 10 pages, 2018.

[28] B. H. Osman, X. Sun, Z. Tian, H. Lu, and G. Jiang, "Dynamic compressive and tensile characteristics of a new type of ultra-high-molecular weight polyethylene (UHMWPE) and polyvinyl alcohol (PVA) fibers reinforced concrete," *Shock and Vibration*, vol. 2019, Article ID 6382934, 19 pages, 2019.

[29] A. Reyes-Salazar, E. Bojórquez, Juan Bojorquez, F. Valenzuela-Beltran, and M. D. Llanes-Tizoc, "Energy dissipation and local, story, and global ductility reduction factors in steel frames under vibrations produced by earthquakes," *Shock and Vibration*, vol. 2018, Article ID 9713685, 19 pages, 2018.

[30] E. Bojorquez, A. Reyes-Salazar, A. Teran-Gilmore, and S. E. Ruiz, "Energy-based damage index for steel structures," *Steel & Composite structures*, vol. 10, no. 4, pp. 331–348, 2010.

[31] B. Dadfar, M. H. El Naggar, and M. Nastev, "Vulnerability of buried energy pipelines subject to earthquake-triggered transverse landslides in permafrost thawing slopes," *Journal of Pipeline Systems Engineering and Practice*, vol. 9, no. 4, article 04018015, 2018.

[32] N. Bonora, D. Gentile, P. P. Milella, G. Newaz, and F. Iacoviello, "Ductile damage evolution under different strain rate conditions," *ASME*, vol. 246, pp. 145–154, 2000.

[33] L. Susmel, F. Berto, and Z. Hu, "The strain energy density to estimate lifetime of notched components subjected to variable amplitude fatigue loading," *Frattura ed Integrità Strutturale*, vol. 13, no. 47, pp. 383–393, 2019.